ACS APPLIED MATERIALS & INTERFACES

Research Article

www.acsami.org

Nanowire-Functionalized Cotton Textiles

Maksym Zhukovskyi,[†] Lina Sanchez-Botero,[‡] Matthew P. McDonald,[†] Juan Hinestroza,*[,‡] and Masaru Kuno*[,†]

[†]Department of Chemistry and Biochemistry, University of Notre Dame, 251 Nieuwland Science Hall, Notre Dame, Indiana 46556, United States

[‡]Fiber Science and Apparel Design, Cornell University, Ithaca, New York 14850, United States

Supporting Information

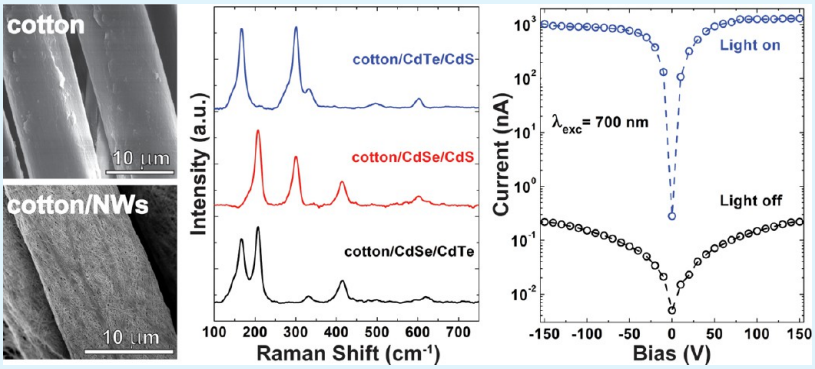

ABSTRACT: We show the general functionalization of cotton fabrics using solution-synthesized CdSe and CdTe nanowires (NWs). Conformal coatings onto individual cotton fibers have been achieved through various physical and chemical approaches. Some involve the electrostatic attraction of NWs to cotton charged positively with a Van de Graaff generator or via 2,3-epoxypropyltrimethylammonium chloride treatments. Resulting NW-functionalized textiles consist of dense, conformal coatings and have been characterized for their UV−visible absorption as well as Raman activity. We demonstrate potential uses of these functionalized textiles through two proof-of-concept applications. The first entails barcoding cotton using the unique Raman signature of the NWs. We also demonstrate the surface-enhancement of their Raman signatures using codeposited Au. A second demonstration takes advantage of the photoconductive nature of semiconductor NWs to create cotton-based photodetectors. Apart from these illustrations, NW-functionalized cotton textiles may possess other uses in the realm of medical, anticounterfeiting, and photocatalytic applications.

KEYWORDS: *CdSe, CdTe, nanowire, cotton fabrics, Raman spectroscopy, photodetector*

INTRODUCTION

Cotton—a natural fiber consisting of 90% cellulose—has been widely used for centuries.[1] To expand its properties and use, numerous studies have since explored functionalizing cotton with different metal,[2,3] semiconductor,[4,5] organic,[6,7] and carbon-based[8,9] materials. Resulting hybrid cotton textiles exhibit enhanced properties and incorporate the unique mechanical, optical, and electrical properties of these systems. As examples, cotton/metal (Ag, Au, Cu, Pd, and Pt) composites possess conductive and/or catalytic properties useful in medical, photocatalytic, and electronic applications.[2] Wide gap semiconductor functionalized cotton (e.g., with TiO_2 or ZnO) show good UV-blocking properties, exhibit self-cleaning behavior, and possess antibacterial properties.[4,5,10] Cotton textiles have even been modified with carbon nanotubes to obtain features such as enhanced mechanical properties, flame retardation, and hydrophobicity.[8,9]

In parallel, semiconductor nanostructures such as quantum dots and nanowires (NWs) possess unique size-dependent optical and electrical properties. This stems from confinement effects that arise when their physical dimensions are smaller than the natural length scales of electrons and holes in these materials.[11] These size-dependent effects make nanostructured materials appealing for various optical,[12] electrical,[13] photovoltaic,[14] and photocatalytic applications.[15] Much of this interest has been spurred by recent synthetic advances that enable one to obtain large yields of highly crystalline nanostructures with controlled sizes, size distributions, and morphologies. In the realm of NWs, solution-liquid−solid (SLS) growth[16] has enabled the facile synthesis of crystalline wires with compositions spanning the II−VI, III−V and IV−VI semiconductor families (e.g., ZnSe,[17] CdSe,[18] CdTe,[19] InP,[16] GaAs,[16] PbS,[20] PbSe,[20] $PbSe_xS_{1-x}$[20]). Resulting diameters are often within the confinement regimes of their respective

Received: July 27, 2013
Accepted: January 28, 2014
Published: January 28, 2014

   dx.doi.org/10.1021/am4052602 | ACS Appl. Mater. Interfaces 2014, 6, 2262−2269

systems, leading to aforementioned size-dependent optical properties.[18] The wires are also passivated with surfactant molecules, making them compatible with industrially relevant solution processing technologies.

In this paper, we demonstrate how cotton can be functionalized with CdSe and CdTe NWs. The technique is general, and can be applied to other NW systems. Various approaches have been used to deposit CdSe and CdTe nanowires onto cotton, taking advantage of the ability to induce large dipoles in them using electric fields. Complementary chemical approaches exploit the ability to chemically cationize cotton fibers. Resulting NW-functionalized cotton fabrics exhibit similar mechanical properties as their non-functionalized counterparts. Furthermore, they are optically active, and exhibit sizable photoconductivities. We demonstrate potential uses for these NW-functionalized textiles through two proof-of-concept applications. The first illustrates the barcoding of cotton using the unique Raman signature of the NWs. The second illustrates how NW photoconductivity can be exploited to make cotton-based photodetectors.

EXPERIMENTAL SECTION

Materials. Cotton fabrics were obtained from a local store. Additional standardized TIC-400 woven cotton fabrics were acquired from Textile Innovators, Inc. (Windsor, NC). 3-chloro-2-hydroxypropyl-trimethylammonium chloride (65% in water) (CHPTAC) was purchased from TCI America. Trioctylphosphine (TOP, 90.0%), pyridine (99.0%), octadecene (ODE, 90.0%), oleic acid (90.0%), cadmium oxide (99.9%+, metal basis), tellurium powder (99.8%), and NaOH crystals were purchased from Sigma Aldrich. Tri-n-octylphosphine oxide (TOPO, 99.0%) was purchased from Strem Chemicals. Bismuth(III) chloride (98.0%), and selenium powder (99.5%) were obtained from Acros. Stearic acid (98.0%) was acquired from Alfa Aesar. Decylphosphonic acid (98.0%) was purchased from PCI synthesis. Acetic acid (99.7%), acetone (99.9%), methanol (99.8%) and toluene (99.5%) were obtained from Fisher Scientific and VWR. All chemicals were used without further purification.

$BiCl_3$ Solution. To initiate NW growth, a Bi catalyst solution is required. A 2 mM $BiCl_3$ solution was therefore prepared by dissolving $BiCl_3$ (12.6 mg, 40 μmol) in 20 mL of acetone.

TOPSe, TOPTe, and TOPS Solutions. Chalcogen sources are required for NW growth. One molar trioctylphosphine selenide (TOPSe) was therefore prepared by mixing selenium powder (0.8 g, 10.0 mmol) and TOP (10.0 mL, 20.2 mmol) under nitrogen. The mixture was then stirred overnight and was stored in a glovebox. One-half molar trioctylphosphine telluride (TOPTe) was likewise prepared by mixing tellurium powder (0.6 g, 5.0 mmol) and TOP (10.0 mL, 20.2 mmol) in a three neck flask connected to a Schlenk line. The mixture was kept under vacuum at 100 °C for 1 h to dry and degas the solvent. Afterward, the flask was backfilled with N_2 and was heated to 170 °C. When the tellurium powder completely dissolved, the solution was cooled to room temperature and was subsequently stored in a glovebox. One molar trioctylphosphine sulfide (TOPS) was prepared by mixing sulfur powder (0.32 g, 10.0 mmol) and TOP (10.0 mL, 20.2 mmol) under nitrogen. The mixture was then stirred overnight and was stored in a glovebox.

Nanowire Synthesis. CdSe, CdTe and CdS NWs were synthesized using SLS growth.[21−23] All NW samples were imaged with a transmission electron microscope (TEM, JEOL). Average diameters and lengths were determined using TEM vendor-provided software (sample size = 100). Corresponding XRD powder patterns of CdSe and CdTe NWs can be found in the Supporting Information, Figure S1. Brief descriptions of NW syntheses follow.

CdSe NWs. CdSe NWs were prepared following the methods described in refs 21 and 22 with some modifications. To make CdSe NWs, we combined TOPO (2.5 g, 6.5 mmol), cadmium oxide (25.0 mg, 0.2 mmol), and stearic acid (0.2 g, 0.7 mmol) in a three-neck flask connected to a Schlenk line. The mixture was stirred under a vacuum at 150 °C for 1 h to dry and degas it. The reaction vessel was backfilled with N_2 and was heated to 350 °C. When the initial red slurry turned clear, the temperature was lowered to 250 °C. An injection solution, consisting of 1 M TOPSe (50.0 μL, 50.0 μmol) and 2 mM $BiCl_3$ in acetone (100.0 μL, 0.2 μmol), was then rapidly introduced into the three-neck flask. A dark-brown solution resulted due to the formation of NWs. The solution was subsequently left at 250 °C for two additional minutes and was cooled to 75 °C to stop the reaction. Toluene (15.0 mL) was added to prevent TOPO from solidifying. Produced NWs were precipitated from suspension by adding an excess of methanol (10.0 mL). The wires were recovered by centrifuging this mixture and were subsequently subjected to several toluene/methanol washing steps to remove any excess TOPO. Resulting NWs were stored in toluene.

CdTe NWs. CdTe NWs were prepared following methods described in refs 21 and 22 with some modifications. TOPO (2.5 g, 6.5 mmol), CdO (25.0 mg, 0.2 mmol) and decylphosphonic acid (70.0 mg, 0.3 mmol) were combined in a three neck flask connected to a Schlenk line. The mixture was stirred under vacuum at 150 °C for 1 h in order to dry and degas it. The reaction vessel was backfilled with N_2 and was heated to 350 °C. The initially red slurry became clear on prolonged heating. At this point, TOP (2.5 mL, 5.1 mmol) was added to the mixture and the temperature was decreased to 285 °C. An injection solution consisting of 0.5 M TOPTe (50.0 μL, 25.0 μmol) and 2 mM $BiCl_3$ in acetone (50.0 μL, 0.1 μmol) was then introduced into the three-neck flask to initiate NW growth. The resulting solution turned dark-brown, indicating the presence of NWs. The mixture was left heating at 285 °C for two additional minutes and was cooled to 75 °C to stop the reaction. Toluene (15.0 mL) was added to prevent TOPO from solidifying whereupon the NWs were precipitated from the mixture by adding an excess of methanol (10.0 mL). The wires were recovered by centrifuging this suspension and were then subjected to several toluene/methanol washing steps to remove any excess surfactant. Obtained NWs were stored in toluene.

CdS NWs. CdS NWs were prepared following the method described in ref 23 with some modifications. TOPO (1.0 g, 2.6 mmol), CdO (64.0 mg, 0.5 mmol), ODE (3 mL, 0.6 mmol) and oleic acid (0.4 mL, 1.3 mmol) were combined in a three neck flask connected to a Schlenk line. The mixture was stirred under vacuum at 150 °C for 1 h in order to dry and degas it. The reaction vessel was backfilled with N_2 and was heated to 315 °C. When the initial red slurry turned clear, an injection solution, consisting of 1 M TOPS (50.0 μL, 50.0 μmol) and 2 mM $BiCl_3$ in acetone (50.0 μL, 0.1 μmol), was rapidly introduced into the three-neck flask to initiate NW growth. The resulting solution turned orange, indicating the presence of NWs. The mixture was left heating at 315 °C for two additional minutes and was cooled to 75 °C to stop the reaction. Toluene (15.0 mL) was added to prevent TOPO from solidifying whereupon the NWs were precipitated from the mixture by adding an excess of methanol (10.0 mL). The wires were recovered by centrifuging this suspension and were subjected to several toluene/methanol washing steps to remove any excess surfactant. Obtained NWs were stored in toluene.

Pyridine Treatment. To improve nanowire transport properties in photoconductivity measurements, we performed ligand exchange to replace TOPO and other insulating surface species with pyridine. NWs were first isolated by centrifuging toluene suspensions. Pyridine (15.0 mL) was then added to the precipitate. The pyridine suspension was stirred at 65 °C for 30 min whereupon NWs were recovered by centrifuging the mixture. This washing procedure with pyridine was carried out three times, with the final precipitate stored in toluene.

Cationization of Cotton. To improve the NW-to-cotton affinity, cotton samples were chemically modified through cationic functionalization. Briefly, under alkaline conditions, ammonium epoxides react with the OH groups of cellulose to create cotton with positively charged surfaces.[6,7] A solution of 2,3-epoxypropyltrimethylammonium chloride (EPTAC) was therefore prepared by reacting 3-chloro-2-hydroxypropyl-trimethylammonium chloride (CHPTAC) with NaOH using the procedure described in refs 6 and 7. The process consists of adding CHPTAC (33.3 g, 0.1 mol) and NaOH (15.2 g, 0.4 mol) to

66.7 mL of deionized water. Cotton fabrics (25 × 25 mm) were immersed into this solution and were recovered when thoroughly soaked. Samples were stored in plastic bags for 24 h at room temperature to complete the reaction. Specimens were subsequently rinsed with dilute acetic acid (17 mM) to neutralize the fabrics and were dried under ambient conditions. Mercerized cotton samples were obtained using an identical procedure but without the use of CHPTAC.

Cotton/NW Composites. NWs were deposited onto cotton textiles using several physical and chemical approaches. Physical approaches: (1) CdSe and CdTe NWs were adsorbed onto cotton by dipping cotton specimens into NW/toluene suspensions (NW concentration ~3.7×10^{-11} M); (2) by irradiating NW suspensions with broadband visible light (196.5 W/cm^2 at 630 nm) during dip-coating; (3) by electrostatically charging cotton fabrics prior to dip-coating using a 25 kV Van de Graaff generator (VDGG) (the resulting average surface voltage of the cotton was ~0.3 kV/cm^2 with a corresponding charge density of 5.8×10^{-11} C/cm^2). Chemical approaches: adsorbing CdSe and CdTe NWs onto (4) mercerized and (5) EPTAC-cationized cotton via dip-coating. For all approaches, dip-coating was carried out once. After dip-coating, cotton/NW samples were allowed to dry overnight under ambient conditions. Digital photographs of the as-produced fabrics can be found in the Supporting Information (Figure S2). Cotton functionalization is not limited to CdSe and CdTe NWs but can also be applied using other 1D nanostructures (such as ZnSe, ZnO, TiO_2, etc.). To highlight this, we deposited ZnSe NWs onto cotton fabrics resulting in dense, conformal coatings. SEM images (see Figure S3 in the Supporting Information) and other details—including the ZnSe NW synthesis—can be found in the Supporting Information.

Characterization. Surface morphologies of bare cotton and NW-functionalized textiles were studied with a field-emission scanning electron microscope (SEM, FEI). Prior to observation, samples were sputter coated with 5 nm of iridium. Raman spectra were collected with a micro Raman spectrometer (Jasco) using 532 nm excitation. Absorption spectra were acquired in reflectance mode with a 60 mm integrating sphere on a Jasco spectrometer. Emission spectra were acquired using a microphotoluminescence setup based around an inverted optical microscope. A detailed description of this system can be found in ref 21. Photocurrent measurements were carried out by applying a bias voltage (+150 V) across Au electrodes (60 μm gap, associated electric field ~2.5×10^4 V/cm; electrodes made by sputtering Au onto a microscope coverslip using a 60 μm copper wire as a shadow mask). Cotton/NW composites were then placed across the electrodes and were held in place with a second (nonpatterned) coverslip. The two coverslips were fastened together using epoxy. Tunable excitation from 450 to 850 nm was obtained from a supercontinuum white light source (Fianium) dispersed with an acousto-optic tunable filter. At a given excitation wavelength, the light was focused onto the sample using a visible achromatic doublet. The incident power on the sample was monitored with a variable wavelength power meter. Associated excitation intensities ranged from ~180 to ~430 mW/cm^2. A digital picoammeter (Kiethley) was used to measure resulting photocurrents.

Wettability. Fabric samples were cut along the warp direction with dimensions of 10 mm (width) × 25 mm (length). Wettability tests were conducted using a commercial tensiometer (KSV Sigma 700). Samples were lowered to the working liquid level with measurements carried out using distilled water as a wetting agent. The vertical wicking behavior of cotton/NW fabrics was determined by taking mass readings of water uptake as a function of time along the fabric's warp direction.

Mechanical Properties. The tensile properties and break point elongation of cotton/NW fabrics were measured using a commercial tensile tester (Instron, model 5566). Fabric dimensions were 28 × 28 mm^2. The instrument gage length was set to 10 ± 1 mm with a corresponding crosshead speed of 10 mm/min. Breaking load, ultimate tensile strength, and ultimate tensile strain were measured along the fabric's warp direction.

Durability Test. Durability tests were conducted on NW treated fabrics following the procedure described in ref 10 with some modifications. Three tests simulating normal garment washing procedures were conducted. In the first, sample swatches were soaked in room temperature DI water for one hour under continuous stirring. The second test involved soaking sample swatches in a 60 °C tap water/detergent solution (1 wt %) for 1 h under continuous stirring. For the third test, sample swatches were soaked in 60 °C DI water for one week under continuous stirring. After soaking, cotton fabrics were rinsed with tap water or DI water and were then dried in open air. Sample quality before and after the durability test was verified using SEM imaging. Additional details, including SEM images and inductively coupled plasma atomic emission spectroscopy (ICP-AES) measurements of the DI water after washing can be found in the Supporting Information, Figure S4.

RESULTS AND DISCUSSION

Figure 1a shows an SEM image of unmodified locally purchased cotton fabric. Surfaces of individual cotton fibers are seen to be smooth. Figure 1b–f shows complementary SEM images of fabrics functionalized with CdSe NWs (images of CdTe-functionalized cotton and additional images of CdSe functionalized cotton are available in the Supporting Information,

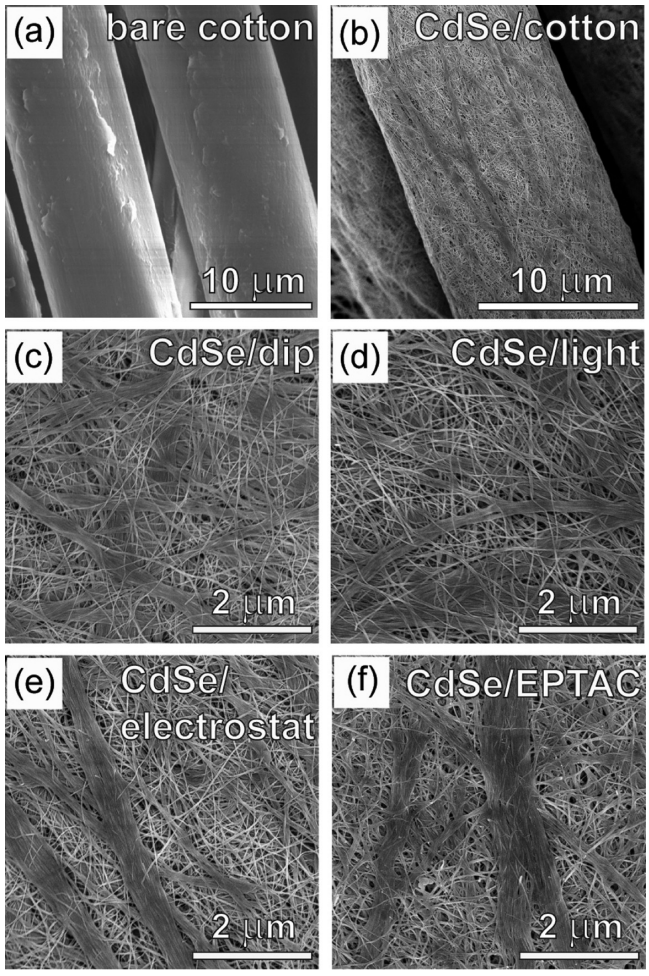

Figure 1. Low-resolution SEM images of (a) locally purchased cotton, and (b) cotton functionalized with CdSe NWs. Corresponding high-resolution SEM images are shown for cotton/CdSe NWs after (c) simple dip-coating deposition, (d) light-induced dip-coating deposition, (e) VDGG stimulated dip-coating deposition, and (f) dip-coating deposition onto cationized cotton.

Figures S5 and S6). In either case, individual cotton fibers exhibit dense, conformal coatings. This is due to the small dimensions of the NWs relative to those of individual cotton fibers. Specifically, average diameters of CdSe (CdTe) NWs are $d = 12.9 \pm 2.3$ nm ($d = 9.9 \pm 1.8$ nm) with lengths $l = 10-15$ μm (see Figure S7 in the Supporting Information), whereas those of individual cotton fibers are $d = 10-12$ μm with lengths up to 1 cm (see Figure S8 in the Supporting Information). Figure 1 also reveals that the deposited NWs form an interlinked network that encapsulates individual cotton fibers. This characteristic could be important for applications involving abrasion and friction resistant cotton textiles. The NW's nanoscale dimensions also mean that cotton's intrinsic mechanical properties are retained.

Figure 1c–f show SEM images of cotton/CdSe NW composites made using different deposition approaches outlined in the Experimental Section. We find that either illuminating NW suspensions with light during dip-coating (Figure 1d) or using a VDGG to charge the cotton (Figures 1e) leads to the apparent formation of macroscopic NW bundles in solution. These bundles subsequently deposit onto cotton fibers. In the former case, we speculate that this agglomeration results from the light-induced dipole–dipole coupling of individual wires, which leads to an increased proclivity for NW bundling prior to deposition. This bundling phenomenon has previously been observed during the light-induced assembly of NW yarns.[21] In the latter case where cotton has been charged with a VDGG prior to dip-coating, resulting electric fields may also enhance the likelihood of NW bundling through a similar mechanism.[24−26] A tendency to form bundles is also observed when cotton is chemically cationized prior to dip-coating (Figure 1f). Analogous results are found for cotton/CdTe NW textiles (see the Supporting Information, Figure S6). In all cases, the NWs form a tight conformal network about individual cotton fibers, with a corresponding NW film thickness of ∼400–700 nm (see the Supporting Information, Figure S9).

To assess the efficiencies of the various deposition approaches, absorption spectroscopy was conducted on functionalized cotton samples. Results are shown in Figure 2a, where absorption spectra of cotton/CdSe NW composites are shown. Solution absorption spectra of CdSe (and CdTe) NWs are provided in Figure S10 of the Supporting Information for comparison purposes. The cotton/CdSe NW fabrics exhibit an absorption onset at 720 nm in agreement with CdSe's bulk band gap of 1.74 eV (∼712 nm).[22] The absorption increases toward higher energies in a manner consistent with the increasing density of states of CdSe NWs. Furthermore, the data show that the amount of light absorbed by the functionalized fabrics increases when the dip-coating method (trace 1) is augmented with concurrent illumination of NW suspensions (trace 2), or by pretreating the dipped cotton with a VDGG (trace 3). We also observe large absorption enhancements using both chemical functionalization approaches for cotton (traces 4 and 5). Of all the approaches investigated, EPTAC-cationized cotton textiles exhibit the largest absorbance values (trace 5). This indicates that NW deposition efficiencies increase as follows (from smallest to largest): dip-coating, light stimulated, VDGG stimulated, mercerized, and EPTAC functionalization.

To further establish the functionalization of cotton with CdSe and CdTe NWs, Raman spectra of cotton/NW composites were acquired. Figure 2b shows Raman data

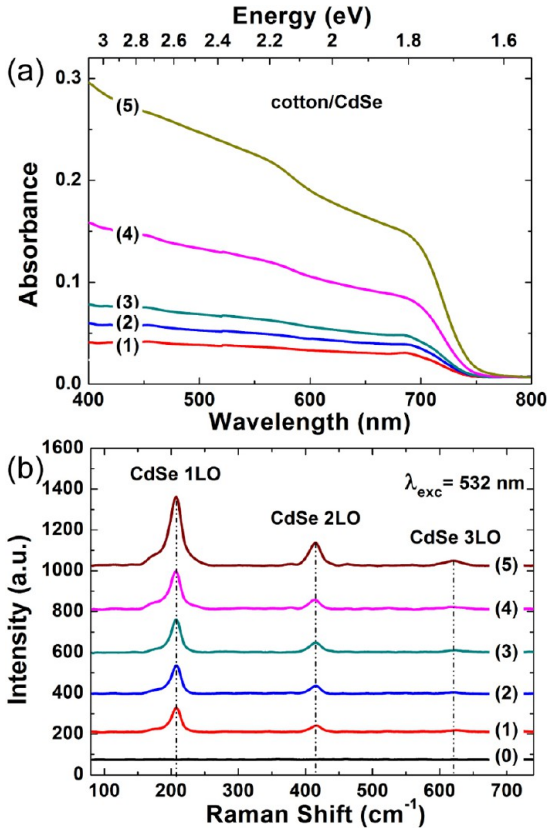

Figure 2. (a) Absorbance spectra of cotton/CdSe NW textiles made with different deposition methods. From bottom to top, the labeled traces are: (1) simple dip-coating deposition of NWs, (2) light-induced dip-coating of NWs, (3) VDGG stimulated dip-coating deposition of NWs, (4) dip-coating deposition of NWs onto mercerized cotton, and (5) dip-coating deposition of NWs onto cationized cotton. (b) Raman spectra of the cotton/CdSe textiles, where numbered labels correspond to the same deposition approaches as in a. For comparison purposes, the Raman spectrum for bare cotton is shown as trace (0). Traces offset for clarity.

taken on cotton/CdSe NW-functionalized textiles. For comparison purposes, the Raman spectrum of bare cotton is shown as trace 0. All cotton/CdSe NW Raman spectra show peaks related to the scattering of CdSe's longitudinal optical (LO) phonons.[27] Specifically, the fundamental peak is observed at 205 cm^{-1}, along with its first (2LO) and second (3LO) overtones (ν_{2LO} = 410 cm^{-1}, ν_{3LO} = 615 cm^{-1}). Analogous results are found for CdTe NW-functionalized fabrics (see the Supporting Information, Figure S11). On the basis of the intensities observed in Figure 2b, these Raman spectra reveal the same trend in NW deposition efficiencies seen earlier in Figure 2a. Namely, deposition efficiencies increase as: dip-coating, light stimulated, VDGG stimulated, mercerized, and EPTAC functionalization (see the Supporting Information, Figure S11). The reproducibility of these Raman results has been confirmed by recording Raman spectra from different locations along functionalized cotton fibers. (See the Supporting Information, Figure S12).

Figure 3 illustrates the water absorbency and mechanical properties (ultimate strain, ultimate strength and load at break) of unmodified cotton fabrics (colored/shaded regions) as well as those of cotton fabrics coated with CdSe (open blue stars) and CdTe (open red squares) nanowires. Water uptake as a function of time can be found in the Supporting Information

dx.doi.org/10.1021/am4052602 | ACS Appl. Mater. Interfaces 2014, 6, 2262–2269

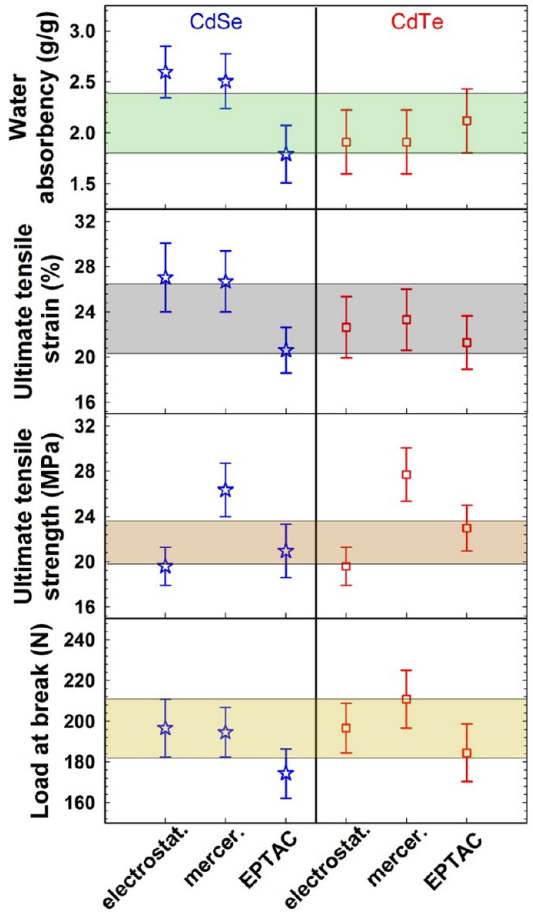

Figure 3. Water absorbency and mechanical properties (ultimate tensile strain, ultimate tensile strength, and load at break) of cotton fibers functionalized with CdSe (open blue stars) and CdTe (open red squares) NWs. Displayed are NW-functionalized textiles obtained using VDGG stimulated dip-coating (electrostat.), dip-coating onto mercerized cotton (mercer.), and dip-coating onto cationized cotton (EPTAC). For comparison purposes, bare cotton's typical range for each property is shown as a colored/shaded region.

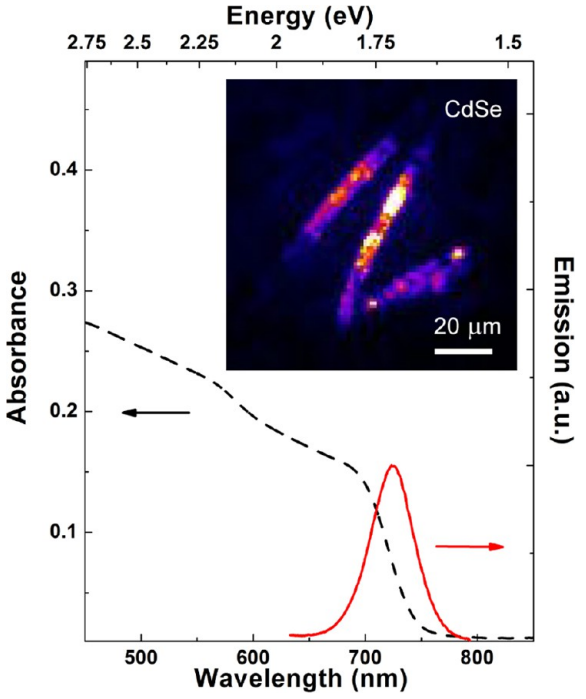

Figure 4. Emission (red solid line) and absorption (black dashed line) spectra of the cotton/CdSe NW composite along with an emission image (false color) of individual CdSe NW-functionalized cotton fibers (inset).

(Figure S13). We find that neither the ability of cotton to absorb water nor the stiffness and extensibility of the fabrics is significantly compromised by the presence of NWs. In addition, durability tests designed to simulate normal garment washing procedures show that cotton/NW composites do not decompose, even after long (i.e., one week) washing periods (see the Experimental Section and the Supporting Information, Figure S4). More information about these durability tests, including ICP-AES measurements of the water after washing, can be found in the Supporting Information.

At the same time, NW-functionalized cotton retains the native optical properties of the deposited wires. Specifically, in addition to the absorption spectra seen previously (Figure 2 and Figure S10 in the Supporting Information), cotton/NW composites exhibit photoluminescence from the wires. Figure 4 shows the corresponding band edge emission of cotton/CdSe NW composites. The inset is a false color emission image of individual cotton/CdSe NW fibers acquired with a micro-photoluminescence setup. No photoluminescence is observed from CdTe samples as emission quantum yields of CdTe NWs are known to be lower than our instrument's detection limit.[19]

Proof-of-Concept Applications. In what follows, we illustrate two proof-of-concept applications using NW-functionalized cotton. The first entails applying the unique Raman spectra of semiconductor NWs to barcode cotton textiles. The second involves taking advantage of NW optical and electrical properties to make cotton-based photodetectors.

Using NW Raman spectra to barcode cotton. We have demonstrated that NW-functionalized cotton textiles readily show Raman spectra characteristic of the deposited wires (Figure 2). By functionalizing EPTAC cotton with a mixture of NW types, cotton textiles can be barcoded and used for identification purposes. This is illustrated in Figure 5 where the Raman spectra of three cotton/mixed-NW composites are shown, specifically, cotton functionalized with a homogeneous mixture (50%/50%) of (1) CdSe + CdTe NWs, (2) CdSe + CdS NWs, and (3) CdS + CdTe NWs. Raman spectra of all three composites show characteristic peaks for both NW species in each mixture. To illustrate, in the case of cotton/CdSe/CdS NW textiles [trace (2)], a set of CdSe peaks at ν_{1LO} = 205 cm^{-1} and ν_{2LO} = 410 cm^{-1} can be seen. Characteristic CdS peaks are also observed at ν_{1LO} = 300 cm^{-1} and ν_{2LO} = 600 cm^{-1}.[28] Analogous responses are seen with cotton/CdSe/CdTe [trace (1)] and cotton/CdTe/CdS textiles (trace 3). For comparison purposes, typical Raman lines of CdS, CdSe, and CdTe are shown as vertical dashed lines. More complex barcodes can be constructed by incorporating additional materials, such as ZnSe NWs (see the Supporting Information, Figure S3). These experiments thus indicate potential uses of cotton/NW functionalization to create fiber-, yarn-, and fabric-based anticounterfeiting systems that protect high-value textile products. Such fabrics could even be applied toward establishing positive identification mechanisms for the military, the police, and first responders.

Next, given that we have previously demonstrated that cotton can be functionalized with Au nanoparticles (NPs),[3] their well-known plasmon resonance can be used to surface-

dx.doi.org/10.1021/am4052602 | ACS Appl. Mater. Interfaces 2014, 6, 2262−2269

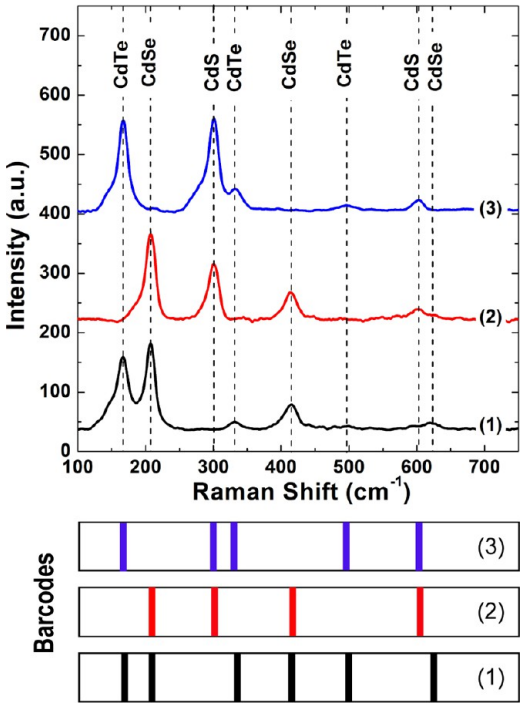

Figure 5. Raman spectra of homogeneously mixed NW-EPTAC functionalized cotton fibers. From bottom to top: (1) cotton/CdSe/CdTe NW, (2) cotton/CdSe/CdS NW, (3) cotton/CdTe/CdS NW. Characteristic Raman lines for CdS, CdSe, and CdTe are shown for comparison purposes. Traces are offset for clarity. Barcodes obtained for each trace are shown below the plot.

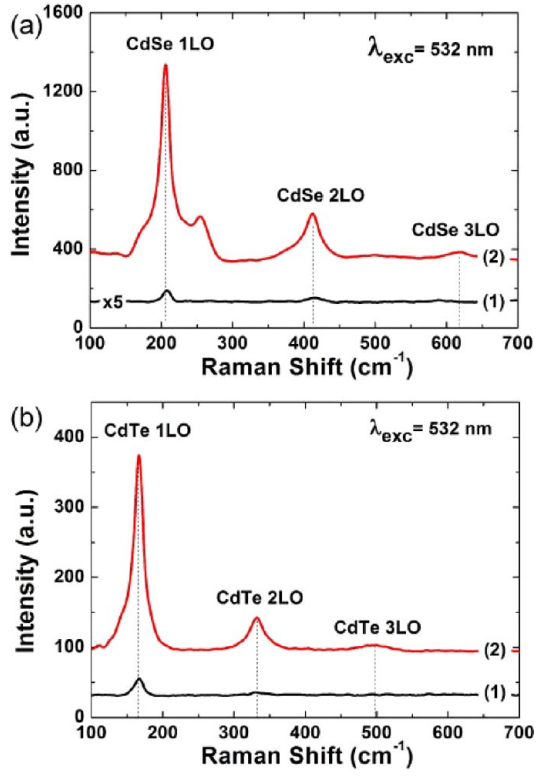

Figure 6. (1) Regular and (2) surface-enhanced Raman spectra of (a) cotton/CdSe NW and (b) cotton/CdTe NW textiles made using dilute NW solutions. Traces are offset for clarity.

enhance the Raman spectra of codeposited NWs. This surface-enhancement effect is an established phenomenon that stems from intense local electric fields at metal surfaces induced by excited surface plasmons.[29] Sizable Raman signals can therefore be obtained from small numbers of analytes, and even from single molecules.[30,31] Within the context of barcoding cotton, surface-enhancements mean that strong Raman signals can be obtained using less NWs, leading to cost-savings in manufacturing. Furthermore, enhanced signals are easier to detect at large distances, allowing for more flexible positive identification mechanisms.

To test the hypothesis, we sputtered a thin film of Au (~100 nm) onto cotton textiles. CdSe and CdTe NWs were then deposited onto these Au-coated cotton fibers through dip-coating. Figure 6 shows resulting Raman spectra of cotton/CdSe NW/Au and cotton/CdTe NW/Au textiles. In either case, CdSe and CdTe LO phonon progressions (first seen in Figure 2 and Figure S11 in the Supporting Information) are apparent. However, the primary difference from the earlier data is that the Raman intensities in Figure 6 are approximately 25 times larger using 8 times less material (see the Supporting Information, Figure S14). This highlights the use of surface enhancements as a cost saving measure, since larger Raman signals are produced using less material (see Figure S15 in the Supporting Information). SEM images of these cotton/NW/Au composites are provided in Figure S16 of the Supporting Information. The data in Figure 6 therefore illustrate not only how cotton textiles cofunctionalized with NWs and Au can be used for barcoding purposes, but more generally, how functionalized cotton acquires the unique optical properties of its adsorbates.

Cotton-Based Photodetector. In our second proof-of-concept application, NW-functionalized cotton yarns were used to demonstrate a cotton-based photodetector. This takes advantage of the photoconductive nature of CdSe NWs.[32,33] Cotton/NW yarns were placed between two gold electrodes with a 60 μm gap. A 150 V bias was applied across the electrodes and photocurrents were measured under illumination (additional details can be found in the Experimental Section). Under exposure to 700 nm light (297.6 mW/cm^2), the conductivities of cotton/NW yarns increase by more than 2 orders of magnitude (from 2×10^{-5} to 6.8×10^{-3} S m^{-1}). After pyridine treatment (Experimental Section), cotton/NW yarn conductivities increase by an additional order of magnitude (to 1.2×10^{-1} S m^{-1}). This is illustrated in Figure 7a. The pyridine treatment enhances the composite's conductivity by removing excess TOPO from NW surfaces. TOPO is known to be an insulating species, which suppresses charge transport in close packed nanostructure films.[21,34]

To ensure that measured photocurrents arise from the deposited NWs, we acquired photocurrent action spectra of cotton/NW composites by scanning the excitation wavelength during measurements. This is illustrated in Figure 7b. The close resemblance of resulting photocurrent action spectra to the absorption of CdSe and CdTe NWs indicates that the wires are responsible for the observed photocurrent. Analogous results have been obtained for cotton/CdSe/CdTe NW yarns, consisting of homogeneously mixed CdSe and CdTe NWs (Figure 7c).

Homogeneously mixed (CdSe/CdTe) NW composites exhibit improved photoconductivities over comparable cotton/CdSe NW and cotton/CdTe NW devices. We attribute this to the enhanced charge separation efficiencies that exist in

dx.doi.org/10.1021/am4052602 | ACS Appl. Mater. Interfaces 2014, 6, 2262−2269

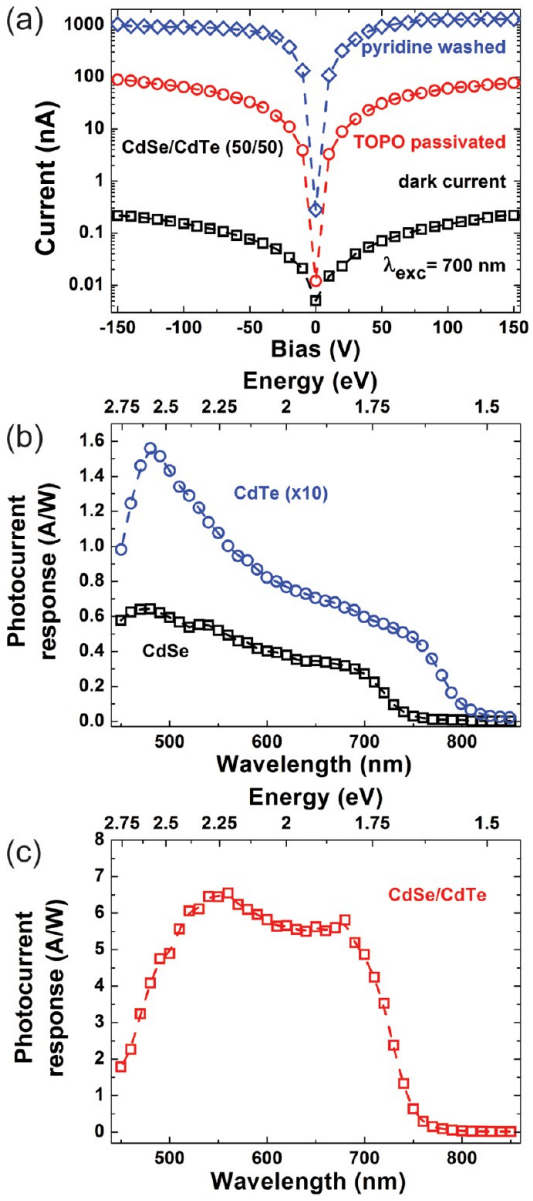

Figure 7. (a) *I*–*V* characteristics and (*b*, *c*) photocurrent action spectra of locally purchased cotton functionalized with: (b) CdSe (open black squares) and CdTe (open blue circles); and (c) homogeneously mixed (50%/50%) CdSe/CdTe NWs. Spectra in b and c were obtained with a +150 V bias.

CdSe/CdTe mixtures, stemming from their mutual Type-II band offsets.[35,36] As a consequence, photogenerated electrons in CdTe migrate into CdSe's conduction band while photogenerated holes in CdSe migrate to CdTe's valence band (see the Supporting Information, Scheme S1). This prevents unwanted electron–hole recombination and better enables the external field to extract both types of charges. Interestingly, we find that the photocurrent response of cotton/CdSe/CdTe NW devices begins around the band edge of CdSe (Figure 7c). This likely implies that photogenerated carriers in CdTe are highly susceptible to trapping into defect states[37] and that further improvements to device performance can be gained by better passivating CdTe's defects.

CONCLUSIONS

We have demonstrated the functionalization of cotton textiles with solution-based semiconductor NWs using various physical and chemical approaches. What results are uniform and conformal coatings, wherein individual cotton fibers are encapsulated by an interlinked NW network. As produced textiles retain cotton's inherent mechanical and absorptive qualities, but are imparted with the unique optical and electrical properties of the NWs. The demonstrated functionalization of cotton is general and NW coatings using other compositions are possible given the solution processability of these wires. Furthermore, two proof-of-concept applications have been demonstrated to illustrate potential uses for these composites. The first entails barcoding cotton using the unique Raman signature of the NWs. A surface-enhancement effect is also demonstrated when Au is codeposited onto cotton, allowing for enhanced Raman signals using significantly lower NW concentrations. The second proof-of-concept application illustrates a cotton-based photodetector which utilizes the intrinsic photoconductivity of CdSe NWs. Beyond these two examples, NW-functionalized cotton may possess other potential uses in areas ranging from anticounterfeiting to positive identification devices.

ASSOCIATED CONTENT

Supporting Information

XRD powder patterns of CdSe and CdTe NWs; digital camera photographs of cotton/CdSe and cotton/CdTe NWs; Raman spectrum and SEM image of cotton functionalized with ZnSe NWs; ZnSe nanowire synthesis; SEM images of EPTAC-cotton/CdSe NW composites before and after durability tests; SEM images of cotton/CdSe and cotton/CdTe NW textiles; TEM images of CdSe, CdTe, and CdS NWs; SEM images of cotton textiles; Cross-sectional SEM images of cotton/CdSe NW composites; Linear absorption spectra of CdSe and CdTe NW solutions and cotton/NW composites; Raman spectra of scientific grade (TIC 400) cotton/CdTe NW textiles; Raman spectra of locally purchased cotton/CdSe NW and cotton/CdTe NW composites taken at 5 separate locations on the functionalized textiles; water absorbency as a function of time for cotton/CdSe NW and cotton/CdTe NW composites; surface-enhanced Raman spectra of cotton/CdSe NW and cotton/CdTe NW textiles made using concentrated NW solutions; correlation in absorbance values and Raman intensities for different deposition approaches; SEM images of cotton/Au and cotton/Au/CdSe NW composites; energy level diagram of CdSe/CdTe composites. This material is available free of charge via the Internet at http://pubs.acs.org.

AUTHOR INFORMATION

Corresponding Authors

*E-mail: jh433@cornell.edu.
*E-mail: mkuno@nd.edu.

Notes

The authors declare no competing financial interest.

ACKNOWLEDGMENTS

M.Z. and M.K. thank the Notre Dame Innovation Postdoc Fund for financial support and the Advanced Electron Microscopy facility of the Notre Dame Integrated Imaging Facility for use of their instrumentation. L.S.-H. and J.H. thank the financial support from the Cornell University Agricultural

Experimental Station federal formula funds, received from the Cooperative State Research, Education, and Extension Service of the U.S. Department of Agriculture. We thank Allen Oliver for aid in XRD measurements, and Dan Klisiewicz for help with sample preparation.

REFERENCES

(1) Ferreira, E. S. B.; Hulme, A. N.; McNab, H.; Quye, A. *Chem. Soc. Rev.* **2004**, *33*, 329−336.
(2) Pinto, R. J. B.; Neves, M. C.; Neto, C. P.; Trindade, T. In *Nanocomposites−New Trends and Developments*; Ebrahimi, F., Ed.; InTech: Rijeka, Croatia, 2012; Vol. *4*, pp 1−24.
(3) Dong, B.; Hinestroza, J. P. *ACS Appl. Mater. Interfaces* **2009**, *1*, 797−803.
(4) Qi, K.; Daoud, W. A.; Xin, J. H.; Mak, C. L.; Tang, W.; Cheung, W. P. *J. Mater. Chem.* **2006**, *16*, 4567−4574.
(5) Wang, L.; Zhang, X.; Li, B.; Sun, P.; Yang, J.; Xu, H.; Liu, Y. *ACS Appl. Mater. Interfaces* **2011**, *3*, 1277−1281.
(6) Hyde, K.; Rusa, M.; Hinestroza, J. *Nanotechnology* **2005**, *16*, S422−S428.
(7) Hauser, P. J.; Taba, A. H. *Color. Technol.* **2001**, *117*, 282−288.
(8) Liu, Y.; Tang, J.; Wang, R.; Lu, H.; Li, L.; Kong, Y.; Qi, K.; Xin, J. H. *J. Mater. Chem.* **2007**, *17*, 1071−1078.
(9) Liu, Y.; Wang, X.; Qi, K.; Xin, J. H. *J. Mater. Chem.* **2008**, *18*, 3454−3460.
(10) Athauda, T. J.; Ozer, R. R.; Chalker, J. M. *RSC Adv.* **2013**, *3*, 10662−10665.
(11) Wang, Y.; Herron, N. *J. Phys. Chem.* **1991**, *95*, 525−532.
(12) Pedrueza, E.; Segura, A.; Abargues, R.; Bailach, J. B.; Chervin, J. C.; Martínez-Pastor, J. P. *Nanotechnology* **2013**, *24*, 205701.
(13) Nah, J.; Kumar, S. B.; Fang, H.; Chen, Y.-Z.; Plis, E.; Chueh, Y.-L.; Krishna, S.; Guo, J.; Javey, A. *J. Phys. Chem. C* **2012**, *116*, 9750−9754.
(14) Nozik, A. J.; Beard, M. C.; Luther, J. M.; Law, M.; Ellingson, R. J.; Johnson, J. C. *Chem. Rev.* **2010**, *110*, 6873−6890.
(15) Abrams, B. L.; Wilcoxon, J. P. *Crit. Rev. Solid State Mater. Sci.* **2005**, *30*, 153−182.
(16) Trentler, T. J.; Hickman, K. M.; Goel, S. C.; Viano, A. M.; Gibbons, P. C.; Buhro, W. E. *Science* **1995**, *270*, 1791−1794.
(17) Petchsang, N.; Shapoval, L.; Vietmeyer, F.; Yu, Y.; Hodak, J. H.; Tang, I.-M.; Kosel, T. H.; Kuno, M. *Nanoscale* **2011**, *3*, 3145−3151.
(18) Kuno, M. *Phys. Chem. Chem. Phys.* **2008**, *10*, 620−639.
(19) Kuno, M.; Ahmad, O.; Protasenko, V.; Bacinello, D.; Kosel, T. H. *Chem. Mater.* **2006**, *18*, 5722−5732.
(20) Onicha, A. C.; Petchsang, N.; Kosel, T. H.; Kuno, M. *ACS Nano* **2012**, *6*, 2833−2843.
(21) Petchsang, N.; McDonald, M. P.; Sinks, L. E.; Kuno, M. *Adv. Mater.* **2013**, *25*, 601−605.
(22) Puthussery, J.; Kosel, T. H.; Kuno, M. *Small* **2009**, *5*, 1112−1116.
(23) Puthussery, J.; Lan, A.; Kosel, T. H.; Kuno, M. *ACS Nano* **2008**, *2*, 357−367.
(24) Zhou, R.; Chang, H.-C.; Protasenko, V.; Kuno, M.; Singh, A. K.; Jena, D.; Xing, H. *J. Appl. Phys.* **2007**, *101*, 073704.
(25) Liu, Y.; Chung, J.-H.; Liu, W. K.; Ruoff, R. S. *J. Phys. Chem. B* **2006**, *110*, 14098−14106.
(26) Freer, E. M.; Grachev, O.; Duan, X.; Martin, S.; Stumbo, D. P. *Nat. Nanotechnol.* **2010**, *5*, 525−530.
(27) Dzhagan, V. M.; Valakh, M. Y.; Raevskaya, A. E.; Stroyuk, A. L.; Kuchmiy, S. Y.; Zahn, D. R. T. *Nanotechnology* **2008**, *19*, 305707.
(28) Suh, J. S.; Lee, J. S. *Chem. Phys. Lett.* **1997**, *281*, 384−388.
(29) Willets, K. A.; Stranahan, S. M.; Weber, M. L. *J. Phys. Chem. Lett.* **2012**, *3*, 1286−1294.
(30) Nie, S.; Emory, S. R. *Science* **1997**, *275*, 1102−1106.
(31) Kneipp, K.; Wang, Y.; Kneipp, H.; Perelman, L. T.; Itzkan, I.; Dasari, R. R.; Feld, M. S. *Phys. Rev. Lett.* **1997**, *78*, 1667−1670.
(32) Lee, S. K. C.; Yu, Y.; Perez, O.; Puscas, S.; Kosel, T. H.; Kuno, M. *Chem. Mater.* **2010**, *22*, 77−84.
(33) Singh, A.; Li, X.; Protasenko, V.; Galantai, G.; Kuno, M.; Xing, H. (G.); Jena, D. *Nano Lett.* **2007**, *7*, 2999−3006.
(34) Yu, D.; Wehrenberg, B. L.; Jha, P.; Ma, J.; Guyot-Sionnest, P. *J. Appl. Phys.* **2006**, *99*, 104315.
(35) Schafer, S.; Reich, A.; Wang, Z.; Kipp, T.; Mews, A. *Appl. Phys. Lett.* **2012**, *100*, 022110.
(36) Gur, I.; Fromer, N. A.; Geier, M. L.; Alivisatos, A. P. *Science* **2005**, *310*, 462−465.
(37) Geyer, S.; Porter, V. J.; Halpert, J. E.; Mentzel, T. S.; Kastner, M. A.; Bawendi, M. G. *Phys. Rev. B: Condens. Matter Mater. Phys.* **2010**, *82*, 155201.